JNeurosci
THE JOURNAL OF NEUROSCIENCE

Research Articles | Systems/Circuits

High-fat diet feeding rapidly induces sex-specific neuronal plasticity in lateral hypothalamic glutamatergic neurons

https://doi.org/10.1523/JNEUROSCI.0781-26.2026

Received: 8 May 2026
Revised: 14 August 2026
Accepted: 14 September 2026

Copyright © 2026 the authors

This Early Release article has been peer reviewed and accepted, but has not been through the composition and copyediting processes.The final version may differ slightly in style or formatting and will contain links to any extended data.

Alerts: Sign up at www.jneurosci.org/alerts to receive customized email alerts when the fully formatted version of this article is published.

Title: High-fat diet feeding rapidly induces sex-specific neuronal plasticity in lateral hypothalamic glutamatergic neurons

Abbreviated title: HFD rapidly induces hypothalamic plasticity

Authors:

Yi Lu[1], Mark A. Rossi[1,2,3,*]

Affiliations:

1 Center for NeuroMetabolism, The Child Health Institute of New Jersey, Rutgers Robert Wood Johnson Medical School, New Brunswick, NJ 08901, USA

2 Department of Neuroscience and Cell Biology, Rutgers Robert Wood Johnson Medical School, New Brunswick, NJ 08901, USA

3 Brain Health Institute, Rutgers University, New Brunswick, NJ 08901, USA

*** Corresponding author:**

Mark A. Rossi, Mark.Rossi@Rutgers.edu

Number of pages: 22

Number of figures: 6

Number of tables: 0

Conflict of interest

The authors declare no competing financial interests.

Acknowledgments

YL designed and performed the research with input from MAR. YL and MAR analyzed the data and wrote the manuscript. We thank Dr. Jorge Luis-Islas and William Meyer for technical assistance and Dr. Zhiping Pang and members of the Rossi lab for comments on earlier drafts of the manuscript. This work was supported by the National Institutes of Health grant #DK136641 (MAR) and Whitehall Foundation grant #2022-12-051 (MAR).

Neurosci Accepted Manuscript

Abstract

Hypothalamic circuits play a central role in coordinating feeding and energy balance, yet how these circuits adapt to dietary excess to regulate body weight remains poorly understood. Lateral hypothalamic area glutamatergic (LHA^{Vglut2}) neurons critically mediate food intake and body weight, but how they adapt their function to acute overfeeding and whether such adaptation is sexually dimorphic are unknown. Here, we examined the impact of high-fat diet (HFD) on LHA^{Vglut2} neurons in mice. Whole-cell recordings revealed baseline sex differences in neuronal properties: female LHA^{Vglut2} neurons exhibited higher basal excitability and differential synaptic input compared to males. HFD feeding produced distinct forms of neuronal plasticity between sexes within 1 day. In males, HFD increased intrinsic excitability while excitatory synaptic input was decreased. In contrast, excitability of female LHA^{Vglut2} neurons remained unchanged, but inhibitory synaptic strength was selectively reduced. To test the causal relationship between enhanced LHA^{Vglut2} neuron excitability and weight gain during overfeeding, we expressed the depolarizing sodium channel NaChBac to chronically increase LHA^{Vglut2} neuron excitability. Chronic elevation of LHA^{Vglut2} neuron excitability suppressed body weight gain during acute HFD exposure in males, whereas females displayed significant weight loss during HFD exposure. Together, these results suggest that female mice may be protected from diet-induced obesity via sexually dimorphic LHA^{Vglut2} neurons. In males, overfeeding rapidly induces compensatory changes in LHA^{Vglut2} neuron excitability that may act to limit body weight gain. Further enhancement of LHA^{Vglut2} neuron excitability can suppress weight gain in an obesogenic environment for both males and females.

Significance Statement

Chronic overeating alters hypothalamic circuits that regulate feeding, but the time course of these adaptations and whether they differ between sexes is poorly understood. Here we show that overeating engages lateral hypothalamic glutamatergic neurons, which negatively regulate food intake and body weight, through sexually dimorphic mechanisms. In males but not females, overfeeding rapidly enhances excitability of lateral hypothalamic glutamatergic neurons. These sex-specific adaptations lead to distinct behavioral outcomes following chronic neuronal activation. Our findings reveal that hypothalamic circuits employ fundamentally different strategies across sexes to respond to dietary excess, providing insight into sex-dependent vulnerability to metabolic disorders.

JNeurosci Accepted Manuscript

Introduction

The hypothalamus plays a central role in the regulation of energy homeostasis by integrating hormonal, nutritional, and neural signals to coordinate feeding behavior and metabolism (Schwartz et al., 2000; Morton et al., 2006). Among hypothalamic nuclei, the lateral hypothalamic area (LHA) has long been recognized as a critical node in the control of feeding and body weight (Anand and Brobeck, 1951; Jennings et al., 2013; Nieh et al., 2015; Rossi, 2023). The LHA contains heterogeneous neuronal populations that regulate energy balance through distinct neurochemical identities and projection targets (Bonnavion et al., 2016; Stuber and Wise, 2016; Rossi and Stuber, 2018; Cheon et al., 2025). In particular, glutamatergic neurons expressing vesicular glutamate transporter 2, Vglut2 (encoded by *Slc17a6*) have emerged as key regulators of feeding and motivated behaviors (Jennings et al., 2013; Nieh et al., 2016; Stamatakis et al., 2016; Lazaridis et al., 2019; Rossi et al., 2019; Siemian et al., 2021b; Shrivastava et al., 2025; Supiot et al., 2026). However, how the activity of these neurons is dynamically regulated by dietary conditions remains incompletely understood.

Exposure to calorie-dense food such as high-fat diet (HFD) can rapidly alter hypothalamic circuit activity and synaptic organization (Pinto et al., 2004; Horvath et al., 2010; Thaler et al., 2012; Zeltser et al., 2012; Stuber et al., 2025). These diet-induced changes are thought to contribute to the neural adaptations that underlie subsequent obesity and metabolic dysfunction. LHA^{Vglut2} neurons negatively regulate feeding wherein bulk chemogenetic or optogenetic activation suppresses food intake (Jennings et al., 2013; Stamatakis et al., 2016). During chronic HFD-induced obesity, their activity is blunted, which is accompanied by transcriptional remodeling (Rossi et al., 2019). This has led to the proposal that LHA^{Vglut2} neurons act as a “brake” on feeding that becomes dysfunctional during obesity. However, because previous studies only measured LHA^{Vglut2} neuron activity after two weeks on HFD, the time course of the neuronal adaptations to HFD is unknown. We therefore aimed to determine how quickly HFD feeding impacts LHA^{Vglut2} neuronal properties.

Accumulating evidence suggests that neural circuits controlling energy balance exhibit pronounced sexual dimorphism. Males and females often respond differently to metabolic challenges, including fasting and overfeeding (Shi and Clegg, 2009; Mauvais-Jarvis, 2015; Godfrey and Borgland, 2020; Massa and Correa, 2020). Female mice often exhibit delayed HFD-induced weight gain compared to males (Hong et al., 2009; Yang et al., 2014; Palmisano et al., 2017). Despite these observations, the cellular mechanisms through which hypothalamic neurons adapt to overconsumption of palatable food in a sex-specific manner remain poorly understood.

JNeurosci Accepted Manuscript

Whether LHA^{Vglut2} neurons undergo sex-dependent intrinsic or synaptic plasticity in response to HFD feeding has not been systematically investigated.

Here, we investigated how HFD feeding influences the physiological properties of LHA^{Vglut2} neurons. Using whole-cell recordings, we identified baseline sex differences in neuronal excitability and inhibitory synaptic input in LHA^{Vglut2} neurons. HFD exposure induced distinct forms of neuronal plasticity between sexes, increasing intrinsic excitability in males while selectively reducing inhibitory synaptic input in females within 1 day. Furthermore, by expressing the depolarizing sodium channel NaChBac to chronically enhance neuronal activity, we demonstrate that activation of LHA^{Vglut2} neurons produces sex- and diet-dependent effects on body weight regulation. These findings reveal sex-specific mechanisms through which hypothalamic circuits adapt to acute overfeeding.

Materials and Methods

Mice

Male and female Vglut2-IRES-Cre mice (C57BL/6 background; Jackson Laboratory, strain #028863) (Vong et al., 2011) were used for all experiments. Mice were housed under a 12 h light/dark cycle with *ad libitum* access to food and water unless otherwise specified. Room temperature was maintained at 21–23 °C with 30–70% humidity. Mice were fed standard chow (Purina 5058; 21% kcal from fat) in their home cages except for HFD experiments in which they received *ad libitum* access to HFD (Bio-Serv #F3282, 60% kcal from fat) in their home cages. All procedures were conducted in accordance with the National Institutes of Health Guide for the Care and Use of Laboratory Animals and were approved by the Rutgers University Institutional Animal Care and Use Committee.

Surgery

Mice were anesthetized with isoflurane (maintained at <1.5%) and positioned in a stereotaxic frame (Kopf Instruments). Ophthalmic ointment was applied to the eyes, and bupivacaine (2 mg/kg) was injected subcutaneously at the incision site. Post-surgery, 5 mg/kg carprofen was administered intraperitoneally. All viruses were delivered through nanoinjectors at a rate of 100 nL/min. Injection coordinates for LHA were (in mm from Bregma): -1.3 Anterior-Posterior; ±1.2 Medial-Lateral; −5.1 Dorsal-Ventral. Injectors were kept in place for at least 10 min after each infusion. Injection sites were confirmed by *post hoc* histological examinations.

JNeurosci Accepted Manuscript

For NaChBac experiments, Vglut2-Cre mice were injected bilaterally with AAV-EF1a-F-FLEX-mNaChBac-T2A-tdTomato (Addgene # v168729, titer: 2.8×10^{12}) and AAV pEF1a-DIO-FLPo-WPRE-hGHpA (Addgene # v102566, titer: 2×10^{13}) (1:1 mix, 300 nL) in LHA. For the control group, Vglut2-Cre mice were injected bilaterally with AAV-EF1a-F-FLEX-mNaChBac-T2A-tdTomato (Addgene # v168729, titer: 2.8×10^{12}) and AAV5-Ef1a-DIO-eYFP (UNC Vector Core, titer: 4.1×10^{12}) (1:1 mix, 250 nL) in LHA. Body weight was measured every day immediately after surgery day.

For patching experiments, Vglut2-Cre mice were injected bilaterally with AAV5- Ef1a-DIO-eYFP (UNC Vector Core, titer: 4.1×10^{12}, 300 nL) in LHA. Mice recovered 2 weeks before testing began. Following recovery from surgery, all animals were singly housed for 1 week before the assay began to reduce potential stress responses. All studies were conducted in a home cage environment with *ad libitum* chow or HFD access.

Open field test

Mice were introduced to the middle of a custom-made 45 × 45 cm square open field arena for 10 min. The mouse's position was tracked from above with a video camera. Mouse position and time spent in the center/peripheral zones were analyzed with custom Python code. The mouse's starting position was defined by the experimenter. Subsequent position is then automatically tracked in each frame by detecting the largest contour and calculating its center of mass. Metrics including the overall distance traversed, duration spent in central versus peripheral areas, and the count of entries into the central zone were calculated. An entry into the center zone was defined as when the center of mass of the animal image enters the center square. Distance travel and time in center zone were calculated with the custom script. Investigators were blinded to the condition during analysis.

Light-dark box test

Light-dark box test was conducted as previously described (Lu et al., 2024). The light–dark box consisted of one dark compartment (6 × 5 × 7 cm) and one illuminated compartment (6 × 5 × 7 cm) connected by a door. At the beginning of the experiments, the animals were individually placed into the light compartment facing the dark compartment and then were allowed to freely explore for 5 min. Time spent in the light zone and number of entries into the light zone were measured using SmartCage tracking system (AfaSci).

Brain slice electrophysiology

JNeurosci Accepted Manuscript

Vglut2-Cre mice that had been surgically injected with AAV5-Ef1a-DIO-eYFP in the LHA were used for LHA recording. Recording was conducted as previously described (Shrivastava et al., 2023; Shrivastava et al., 2025). Three weeks after injections, mice were deeply anesthetized with pentobarbital and then transcardially perfused with ice cold sucrose solution containing in mM: 70 sucrose, 87 NaCl, 2.5 KCl, 1.25 NaH_2PO_4, 25 $NaHCO_3$, 7 $MgCl_2 * 6H_2O$, 0.5 $CaCl_2$, 306–312 mOsm. Brains were rapidly removed, and coronal sections were taken through the LHA at 300 µm. Sections were incubated in artificial cerebrospinal fluid at 32 °C containing in mM: 126 NaCl, 2.5 KCl, 1.2 NaH_2P0_4, 1.2 $MgCl_2$, 26 $NaHCO_3$, 15 glucose, and 2.4 $CaCl_2$; 299–303 mOsm. Cells were visualized with a 40X objective under differential interference contrast imaging on a BX51 (Olympus) microscope. Data were acquired with an EPC 10 recording system running Patchmaster software (Heka Elektronik) at 20 kHz and bandwidth filtered with a 10 kHz Bessel filter and gain 10. Cells were excluded from all analyses if they exhibited unstable access resistance or died during recording. For HFD recordings, mice recovered from viral injection surgery for ~2 weeks before being switched from chow to HFD. Recordings were made from *ad libitum* fed animals after 1-, 2-, and 7 days on HFD.

Current-clamp recordings

Whole-cell current-clamp recordings were used to measure LHA^{Vglut2} neuron excitability. Borosilicate pipettes were pulled to 4–8 MΩ and backfilled with solution containing in mM: 135 potassium gluconate, 10 HEPES, 4 KCl, 4 Mg-ATP, and 0.3, Na-GTP (pH 7.35, 285 mOsm). eYFP-expressing LHA neurons were patched. Current was injected to hold cells at -70 mV. A current ramp of +200 pA over 10 s was used to assess rheobase. Action potential characteristics, including action potential threshold, full width at half maximum (FWHM), afterhyperpolarization (AHP) amplitude, and rise time were calculated from the first or second spike elicited during the rheobase recording. Square pulses of current (500 ms duration, −100 to +300 pA in 20 pA steps) were injected. Evoked spikes for each step were manually counted offline in Patchmaster. Input resistance was calculated as the slope of the I-V curve from -100 to 0 pA current injections. Finally, following the current-step and rheobase protocols, spontaneous firing and resting membrane potential were recorded for 1 min under the zero-current condition (I = 0 pA).

Voltage-clamp recordings

Spontaneous synaptic current recordings were performed in a separate cohort of mice from those used for intrinsic excitability measurements. Whole-cell voltage-clamp recordings were used to assess spontaneous synaptic input onto LHA^{Vglut2} neurons. Borosilicate pipettes were pulled to 4–8 MΩ and backfilled with solution containing in mM: 117 Cs-Methanesulfonate, 20 HEPES, 0.4

JNeurosci Accepted Manuscript

EGTA, 2.8 NaCl, 5 TEA, 5 Mg-ATP, and 0.5 Na-GTP (pH 7.35, 285 mOsm). Cells were held at −70 mV to evaluate EPSCs and +10 mV to evaluate IPSCs. Spontaneous EPSCs and IPSCs were recorded and analyzed offline with Clampfit (Molecular Devices).

Histology

Following completion of behavioral experiments, mice were deeply anesthetized with >250 mg/kg pentobarbital (i.p.) and then transcardially perfused with ice-cold phosphate buffered saline followed by 4% paraformaldehyde. Brains were post-fixed in PFA for 24 h. Sections were taken at 50 µm with a cryostat and mounted onto microscope slides with Fluoroshield mounting medium containing DAPI (ImmunoBioScience). Images were acquired with a Zeiss 700 confocal microscope. Minor adjustments to brightness and contrast for display purposes were made using ImageJ.

Statistical analysis

Electrophysiological data were exported from Patchmaster (Heka) for offline analysis. Excitability data were analyzed using custom Python code to identify action potential characteristics and count spikes. Spontaneous IPSCs and EPSCs were identified and quantified using Clampfit v11.0.3 (Molecular Devices). Statistical analyses were performed with GraphPad Prism (v11.0.2). All statistical tests were two-sided. Specific statistical tests are described in figure legends. For multiple comparisons, Sidak's *post hoc* test was applied where appropriate. Data are presented as mean ± SEM.

RESULTS

Sex differences in excitability and synaptic input of LHA^{Vglut2} neurons

To examine the electrophysiological properties of male and female LHA^{Vglut2} neurons, we performed whole-cell patch clamp recordings from eYFP-labeled neurons in Vglut2-Cre mice after viral targeting of the LHA (**Fig. 1A and B**). LHA^{Vglut2} neurons recorded from *ad libitum* chow-fed female mice fired more action potentials in response to depolarizing current injections than those recorded from males (**Fig. 1C**). This was driven by a reduction in action potential width as measured by the full width at half maximum (FWHM) in females (**Fig. 1D**).

To determine whether this sex difference reflected broader changes in membrane properties, we analyzed additional intrinsic parameters of recorded cells. Action potential threshold (**Fig. 1E**) and rise time (**Fig. 1F**) were similar between males and females. We observed a trend toward reduced

JNeurosci Accepted Manuscript

afterhyerpolarization amplitude in females (**Fig. 1G**), which is consistent with higher firing rates. Resting membrane potential (**Fig. 1H**), input resistance (**Fig. 1I**), spontaneous spike rate (**Fig. 1J**), and rheobase (**Fig. 1K)** were not significantly different between sexes. Together, these results indicate that the higher firing output in females was not accompanied by gross differences in intrinsic cell properties.

We next examined spontaneous synaptic inputs onto LHA^{Vglut2} neurons. Spontaneous excitatory postsynaptic current (EPSC) rate and amplitude were similar between males and females (**Fig. 1L-N**). In contrast, females exhibited a higher spontaneous inhibitory postsynaptic current (IPSC) frequency, whereas IPSC amplitude was unchanged (**Fig. 1O-Q**). Thus, at baseline, female LHA^{Vglut2} neurons display greater evoked firing together with stronger inhibitory synaptic input.

HFD rapidly enhances excitability of LHA^{Vglut2} neurons in males but not females

Because chronic HFD consumption is associated with reduced LHA^{Vglut2} neuron excitability (Rossi et al., 2019), we next aimed to determine how quickly HFD can alter LHA^{Vglut2} neuron properties. To do so, male mice were given *ad libitum* HFD access for 1-, 2-, or 7-days prior to performing excitability recordings (**Fig. 2A-B**). In contrast to chronic HFD consumption, HFD feeding rapidly increased LHA^{Vglut2} neuron excitability in males within 1 day. Action potential firing in response to depolarizing current injection was increased relative to chow-fed controls, with clear enhancement evident after 1-, 2-, and 7-days of HFD exposure (**Fig. 2C and 2D**). Consistent with this, rheobase was significantly reduced after 1-, 2-, and 7-days of HFD in males (**Fig. 2E and 2F**). HFD feeding induced a significant reduction in spike threshold, whereas other membrane and spike-related parameters, including FWHM, resting membrane potential, input resistance, and spontaneous firing rate were unaffected (**Fig. 2F-J**).

By contrast, female LHA^{Vglut2} neurons did not show a comparable increase in firing across HFD conditions (**Fig. 3A-B**). Spiking evoked by depolarizing current injections (**Fig. 3C-D**) and rheobase (**Fig. 3E-3F**) remained unchanged after 1-, 2-, and 7-days of HFD consumption in females. As in males, we observed a modest reduction in the spike threshold in the first 2 days of HFD consumption that was eliminated by day 7. Similarly, in females, other membrane and spike-related parameters, including FWHM, resting membrane potential, input resistance, and spontaneous firing rate were unaffected by HFD consumption (**Fig. 3F-J**). Together, these data indicate that HFD rapidly increases LHA^{Vglut2} neuron excitability in males but not in females.

JNeurosci Accepted Manuscript

HFD sex-dependently remodels excitatory and inhibitory synaptic inputs onto LHA^{Vglut2} neurons

Because HFD feeding rapidly enhanced LHA^{Vglut2} neuron excitability in males but not females, we next tested whether diet also affects synaptic input onto LHA^{Vglut2} neurons. Synaptic input was measured after 1-, 2-, and 7-days of HFD feeding. In males, HFD feeding reduced the frequency of spontaneous EPSCs onto LHA^{Vglut2} neurons (**Fig. 4A-B**), whereas EPSC amplitude remained unchanged (**Fig. 4C**). In contrast, HFD feeding did not alter IPSC frequency or amplitude of LHA^{Vglut2} neurons relative to chow feeding (**Fig. 4D-F**). These findings suggest that, in males, acute HFD consumption is associated with reduced excitatory synaptic drive onto LHA^{Vglut2} neurons.

The impact of acute HFD feeding on female LHA^{Vglut2} neurons is distinct from that of males. In contrast to males, HFD did not significantly alter EPSC frequency or amplitude in females (**Fig. 4G-I**). However, IPSC frequency was markedly reduced after 1- and 2-days of HFD feeding, with no significant difference evident by day 7, suggesting a transient suppression of synaptic input onto female LHA^{Vglut2} neurons. IPSC amplitude was markedly reduced after 1 day of HFD feeding, but no significant difference is evident at days 2 and 7 (**Fig. 4J-L**). Thus, in females, HFD transiently reduces inhibitory synaptic input onto LHA^{Vglut2} neurons rather than changing excitatory drive.

Taken together, these data show that HFD is associated with rapid and distinct electrophysiological changes in male and female LHA^{Vglut2} neurons. Males exhibit enhanced excitability accompanied by reduced excitatory synaptic input, whereas females exhibit reduced inhibitory synaptic tone without a detectable increase in excitability.

Chronic activation of LHA^{Vglut2} neurons produces sex- and diet-dependent effects on body weight and food intake

The observed increase in male LHA^{Vglut2} neuron excitability in response to acute HFD feeding contrasts with results from chronic HFD tests, which suppress LHA^{Vglut2} neuron activity (Rossi et al., 2019). We thus hypothesized that increased excitability after HFD feeding may be a compensatory mechanism by which the brain attempts to restrain weight gain in an obesogenic environment. Alternatively, although unlikely given its established role in feeding suppression (Jennings et al., 2013; Stamatakis et al., 2016; Rossi et al., 2019), increased LHA^{Vglut2} neuron activity may cause weight gain in an obesogenic environment. To test these possibilities, we

JNeurosci Accepted Manuscript

expressed the sodium channel from bacteria, NaChBac, in LHA^{Vglut2} neurons, which chronically elevates neuronal excitability (**Fig. 5A**) (Xue et al., 2014; Ubina et al., 2021). Electrophysiological validation confirmed that NaChBac significantly increased excitability by reducing the rheobase (**Fig. 5B**) and hyperpolarizing the action potential threshold (**Fig. 5C**). In agreement with previous reports (Sim et al., 2013), NaChBac-expressing cells exhibited long-lasting depolarizations in response to current injections (**Fig. 5D**). No sex differences were observed across these parameters, suggesting that excitability was increased similarly in male and female LHA^{Vglut2} neurons.

We next monitored body weight changes over the first 7 days after NaChBac injection surgery under chow- or HFD-maintained conditions. In male mice, NaChBac attenuated body weight gain under both chow and HFD conditions, with significant differences emerging at later post-surgical time points (**Fig. 5E,F & 5I,J**). In contrast, in female mice, NaChBac had little effect on body weight under chow conditions (**Fig. 5G,H**), but markedly suppressed body weight gain under HFD conditions (**Fig. 5K-N**). These results indicate that increasing LHA^{Vglut2} neuron excitability is sufficient to alter body weight regulation in a sex- and diet-dependent manner and indicate that increased excitability observed during HFD acts to counteract the effects of HFD rather than to facilitate weight gain.

To further examine the behavioral consequences of NaChBac activation, we measured acute food intake in different dietary contexts. In chow-maintained mice, NaChBac did not significantly alter 6-hour food intake in either males or females (**Fig. 5O**). However, NaChBac significantly increased HFD intake in both males and females that were maintained on HFD prior to testing (**Fig. 5P**). Thus, NaChBac-mediated activation did not reduce food intake despite suppressing body weight gain, suggesting that suppression of weight gain is driven by increased energy expenditure and not by reduced food intake.

Finally, to test whether changes in body weight were caused by altered anxiety-like behavior or locomotion, we performed light-dark box and open field tests. In the light-dark box, NaChBac expression did not significantly alter time spent in the light (anxiogenic) zone or entries into the light zone in either males or females (**Fig. 6A-B**). Similarly, NaChBac had no effect on time spent in the center of the open field arena or total distance covered (**Fig. 6C-D**) in either males or females. Together, these results indicate that NaChBac expression in LHA^{Vglut2} neurons does not significantly alter anxiety-like behavior or locomotor activity in either sex.

JNeurosci Accepted Manuscript

Discussion

We identified rapid sex-specific electrophysiological adaptations of LHA^{Vglut2} neurons to HFD overfeeding and linked these adaptations to behavioral consequences of chronic neuronal activation. On chow, female LHA^{Vglut2} neurons exhibited greater evoked firing and received stronger inhibitory synaptic input than in males. Following only 1 day of HFD feeding, male LHA^{Vglut2} neurons showed enhanced excitability, while female neurons showed reduced inhibitory synaptic input without altered excitability. Increasing intrinsic excitability with NaChBac was sufficient to modify body weight in a sex- and diet-dependent manner while selectively increasing HFD intake. Together, these findings support the idea that LHA^{Vglut2} neurons are physiologically distinct in males and females and respond differentially to overfeeding to regulate body weight in an obesogenic environment.

LHA^{Vglut2} neurons play important roles in feeding suppression, aversion, and energy balance. Interestingly, we observe sexually dimorphic LHA^{Vglut2} neuron excitability under baseline chow-fed conditions. LHA^{Vglut2} neurons, which suppress weight gain, are more excitable in females than in males. This is consistent with previously demonstrated sexual dimorphism at multiple levels, including synaptic organization, intrinsic excitability, and hormonal regulation (Shi and Clegg, 2009; Beery and Zucker, 2011; Mauvais-Jarvis, 2015). Female C57BL6 mice often exhibit delayed HFD-induced weight gain compared to males (Hong et al., 2009; Yang et al., 2014; Palmisano et al., 2017). Increased LHA^{Vglut2} neuron excitability may contribute to this relative resistance to weight gain in an obesogenic environment. Similarly, in contrast to males, female LHA^{Vglut2} neurons did not show pronounced changes in excitability during acute HFD feeding. Females maintained high excitability throughout 7 days of HFD feeding, suggesting that they may resist weight gain through highly excitable LHA^{Vglut2} neurons.

LHA^{Vglut2} neurons comprise distinct subpopulations, some of which have been electrophysiologically profiled. For example, orexin/hypocretin and MCH neurons exhibit differential electrophysiological characteristics. Orexin neurons have high basal firing rates and exhibit a sag upon hyperpolarizing current injection, whereas MCH neurons are quiescent in awake animals (Eggermann et al., 2003; Toossi et al., 2016). Additionally, LHA parvalbumin neurons are distinctly fast-spiking (Kisner et al., 2018). Such electrophysiological diversity is consistent with transcriptomic studies distinct glutamatergic LHA subpopulations, though each subpopulation represents only a small fraction of the total LHA^{Vglut2} population (Mickelsen et al., 2019; Rossi et al., 2019; Rossi et al., 2021). Female LHA^{Vglut2} neurons exhibited greater evoked firing and narrower action potentials than those in males, whereas most membrane properties

Neurosci Accepted Manuscript

and action potential characteristics were comparable between sexes. These properties do not clearly correspond to a previously defined LHA neuronal population. Rather, sex differences may arise from intrinsic properties within one or more LHA^{Vglut2} subpopulation, differences in the relative representation of distinct subpopulations, or both. Studies combining multidimensional molecular identification with electrophysiological characterization are required to distinguish these possibilities. We measured spontaneous firing and resting membrane potential under zero holding current after completing current-step and ramp protocols. Because membrane properties may rapidly undergo activity-dependent adaptations, we cannot exclude the possibility that the preceding stimulation protocols influenced our measurements.

The sex difference in LHA^{Vglut2} neuron excitability is unlikely to arise from changes to synaptic input since we observed only an increase in inhibitory input in females with no changes in excitatory input. Ovariectomizing female mice causes rapid and substantial weight gain that resembles HFD-fed males (Hong et al., 2009). We therefore expect that increased LHA^{Vglut2} neuron excitability in females is caused either directly or indirectly by estrogen signaling. Estrogen receptors are broadly expressed throughout the hypothalamus (Zuloaga et al., 2014) and can modulate neuronal excitability (McHenry et al., 2017), but further studies are needed to clarify whether estrogen acts directly on LHA^{Vglut2} neurons.

We observed that HFD feeding rapidly causes distinct synaptic tuning in males and females. HFD reduced excitatory synaptic input onto male LHA^{Vglut2} neurons. In contrast, female LHA^{Vglut2} neurons showed no change in excitatory input but exhibited reduced inhibitory input during HFD feeding. This suggests that intrinsic mechanisms may dominate the overall output of male LHA^{Vglut2} neurons on HFD, potentially accompanied by additional compensatory changes in synaptic input. In contrast, HFD did not significantly alter excitability but instead reduced inhibitory synaptic input in females, consistent with a disinhibition mechanism. These findings align with observations that HFD rapidly alters hypothalamic function via synaptic remodeling, inflammatory signaling, and neuronal activity (Horvath et al., 2010; Thaler et al., 2012; Valdearcos et al., 2015; Timper and Bruning, 2017). Our data extend these observations by demonstrating that the direction and mechanism of plasticity differ between sexes in LHA^{Vglut2} neurons.

LHA^{Vglut2} neurons receive excitatory input from multiple brain regions including the ventromedial hypothalamus and parabrachial nucleus and inhibitory input from the bed nucleus of the stria terminalis and arcuate nucleus. Future studies can establish whether distinct input pathways are affected by HFD feeding and are sexually dimorphic. Our data also suggest that local circuit

Neurosci Accepted Manuscript

mechanisms may selectively influence body weight while preserving feeding behavior (Lu et al., 2024). Future studies can examine local connectivity of LHA^{Vglut2} neurons.

LHA^{Vglut2} neurons are less active and excitable after long-term HFD feeding in males (Rossi et al., 2019). However, it was unclear when the food-induced neuronal plasticity arises. We were surprised to find that HFD feeding increased male LHA^{Vglut2} neuron excitability within 1 day. The transition from increased excitability during acute HFD exposure to reduced activity after prolonged HFD feeding may reflect homeostatic adaptations that develop in response to sustained changes in neuronal activity. Neurons can homeostatically adjust both their intrinsic excitability and synaptic strength to stabilize activity in response to prolonged perturbations (Turrigiano et al., 1998; Desai et al., 1999). Early increases in LHA^{Vglut2} neuron excitability may subsequently recruit compensatory intrinsic or synaptic mechanisms that reduce neuronal output during prolonged HFD exposure. Longitudinal monitoring studies linking acute and chronic HFD exposure are required to test this possibility.

Our results suggest that increased LHA^{Vglut2} neuron excitability arising during acute HFD exposure is a compensatory mechanism that can restrain weight gain in an obesogenic environment. To test this, we used NaChBac to chronically elevate intrinsic excitability of LHA^{Vglut2} neurons, which suppressed weight gain in a sex- and diet-dependent manner. In males, NaChBac attenuated body weight gain under both chow and HFD conditions, whereas in females, the effect on body weight only manifested under HFD conditions. This confirms that increased LHA^{Vglut2} neuron excitability does not cause weight gain but rather protects against it. Interestingly, expressing NaChBac in female LHA^{Vglut2} neurons did not produce weight loss when mice were on a chow diet. This may be because female LHA^{Vglut2} neurons have enhanced excitability under baseline conditions and are therefore already protected from weight gain. However, NaChBac prevented HFD-induced weight gain for both males and females despite increased HFD intake. This suggests that elevating LHA^{Vglut2} neuron excitability can protect against diet-induced obesity without promoting starvation. Interestingly, NaChBac did not significantly impact locomotion or anxiety-like behavior and increased HFD intake, indicating that suppression of weight gain is likely caused by increased metabolic rate.

Acute optogenetic or chemogenetic LHA^{Vglut2} neuron activation suppresses food intake and is aversive. Conversely, LHA^{Vglut2} neuron ablation promotes hyperphagia and weight gain only when mice have access to highly palatable food (Stamatakis et al., 2016; Shrivastava et al., 2025). Thus, acute manipulations of LHA^{Vglut2} neuron activity affect intake of any food, whereas chronic LHA^{Vglut2} neuron manipulations appear to selectively influence intake of highly palatable food.

Neurosci Accepted Manuscript

Consistent with this, chronic LHA^{Vglut2} neuron stimulation with NaChBac selectively increased HFD but not chow intake. This contrasts with feeding suppression seen with acute LHA^{Vglut2} neuron excitation. Enhanced HFD intake may be caused by circuit level changes induced by chronic LHA^{Vglut2} neuron stimulation. This may be driven by long-term synaptic changes that are not observed during acute manipulations.

Several limitations of the present study should be considered. While we identify sex-specific excitability and synaptic changes, the source of these changes is unknown. Because spontaneous synaptic currents reflect both action potential-dependent and -independent events, we cannot distinguish whether the observed changes in event frequency arise from altered presynaptic excitability, changes in synaptic connectivity, or release probability. Relative contributions of local and long-range inputs onto LHA^{Vglut2} neurons are also unknown. Future studies using miniature synaptic current recordings, paired-pulse analyses, and circuit-specific approaches are required to distinguish between these possibilities. In addition, the LHA^{Vglut2} population is highly heterogeneous, and our recordings do not distinguish among molecularly or projection-defined subpopulations. The sample sizes for the spontaneous EPSC and IPSC experiments were also smaller than those for the intrinsic excitability analyses, which may prevent identification of subpopulation-specific changes in synaptic transmission. Additional studies targeting defined LHA^{Vglut2} subpopulations may determine circuit-specific mechanisms underlying these effects. Finally, prolonged NaChBac-induced depolarization could lead to depolarization block. Although we observed increased intrinsic excitability ex vivo, we cannot exclude the possibility that chronic NaChBac expression causes additional adaptations in vivo.

In summary, male and female LHA^{Vglut2} neurons are regulated through distinct mechanisms during dietary challenge. These sex-specific mechanisms provide a framework for understanding how hypothalamic circuits adapt to obesogenic diets and may contribute to sex differences in metabolic regulation.

JNeurosci Accepted Manuscript

References

Anand BK, Brobeck JR (1951) Localization of a "feeding center" in the hypothalamus of the rat. Proceedings of the Society for Experimental Biology and Medicine Society for Experimental Biology and Medicine 77:323-324.

Beery AK, Zucker I (2011) Sex bias in neuroscience and biomedical research. Neuroscience and biobehavioral reviews 35:565-572.

Bonnavion P, Mickelsen LE, Fujita A, de Lecea L, Jackson AC (2016) Hubs and spokes of the lateral hypothalamus: cell types, circuits and behaviour. The Journal of physiology 594:6443-6462.

Cheon DH, Park S, Park J, Koo M, Kim HH, Han S, Choi HJ (2025) Lateral hypothalamus and eating: cell types, molecular identity, anatomy, temporal dynamics and functional roles. Exp Mol Med 57:925-937.

Desai NS, Rutherford LC, Turrigiano GG (1999) Plasticity in the intrinsic excitability of cortical pyramidal neurons. Nature neuroscience 2:515-520.

Eggermann E, Bayer L, Serafin M, Saint-Mleux B, Bernheim L, Machard D, Jones BE, Muhlethaler M (2003) The wake-promoting hypocretin-orexin neurons are in an intrinsic state of membrane depolarization. J Neurosci 23:1557-1562.

Garcia A, Coss A, Luis-Islas J, Puron-Sierra L, Luna M, Villavicencio M, Gutierrez R (2020) Lateral Hypothalamic GABAergic Neurons Encode and Potentiate Sucrose's Palatability. Front Neurosci 14:608047.

Godfrey N, Borgland SL (2020) Sex differences in the effect of acute fasting on excitatory and inhibitory synapses onto ventral tegmental area dopamine neurons. J Physiol 598:5523-5539.

Hong J, Stubbins RE, Smith RR, Harvey AE, Nunez NP (2009) Differential susceptibility to obesity between male, female and ovariectomized female mice. Nutr J 8:11.

Horvath TL, Sarman B, Garcia-Caceres C, Enriori PJ, Sotonyi P, Shanabrough M, Borok E, Argente J, Chowen JA, Perez-Tilve D, Pfluger PT, Bronneke HS, Levin BE, Diano S, Cowley MA, Tschop MH (2010) Synaptic input organization of the melanocortin system predicts diet-induced hypothalamic reactive gliosis and obesity. Proc Natl Acad Sci U S A 107:14875-14880.

Jennings JH, Rizzi G, Stamatakis AM, Ung RL, Stuber GD (2013) The inhibitory circuit architecture of the lateral hypothalamus orchestrates feeding. Science 341:1517-1521.

Jennings JH, Ung RL, Resendez SL, Stamatakis AM, Taylor JG, Huang J, Veleta K, Kantak PA, Aita M, Shilling-Scrivo K, Ramakrishnan C, Deisseroth K, Otte S, Stuber GD (2015) Visualizing hypothalamic network dynamics for appetitive and consummatory behaviors. Cell 160:516-527.

Kisner A, Slocomb JE, Sarsfield S, Zuccoli ML, Siemian J, Gupta JF, Kumar A, Aponte Y (2018) Electrophysiological properties and projections of lateral hypothalamic parvalbumin positive neurons. PloS one 13:e0198991.

Lazaridis I, Tzortzi O, Weglage M, Martin A, Xuan Y, Parent M, Johansson Y, Fuzik J, Furth D, Fenno LE, Ramakrishnan C, Silberberg G, Deisseroth K, Carlen M, Meletis K (2019) A hypothalamus-habenula circuit controls aversion. Mol Psychiatry 24:1351-1368.

Linehan V, Hirasawa M (2018) Electrophysiological Properties of Melanin-Concentrating Hormone and Orexin Neurons in Adolescent Rats. Front Cell Neurosci 12:70.

Lu Y, Wang L, Luo F, Savani R, Rossi MA, Pang ZP (2024) Dorsolateral septum GLP-1R neurons regulate feeding via lateral hypothalamic projections. Mol Metab 85:101960.

Massa MG, Correa SM (2020) Sexes on the brain: Sex as multiple biological variables in the neuronal control of feeding. Biochim Biophys Acta Mol Basis Dis 1866:165840.

Mauvais-Jarvis F (2015) Sex differences in metabolic homeostasis, diabetes, and obesity. Biol Sex Differ 6:14.

JNeurosci Accepted Manuscript

McHenry JA, Otis JM, Rossi MA, Robinson JE, Kosyk O, Miller NW, McElligott ZA, Budygin EA, Rubinow DR, Stuber GD (2017) Hormonal gain control of a medial preoptic area social reward circuit. Nature neuroscience 20:449-458.
Mickelsen LE, Bolisetty M, Chimileski BR, Fujita A, Beltrami EJ, Costanzo JT, Naparstek JR, Robson P, Jackson AC (2019) Single-cell transcriptomic analysis of the lateral hypothalamic area reveals molecularly distinct populations of inhibitory and excitatory neurons. Nat Neurosci 22:642-656.
Morton GJ, Cummings DE, Baskin DG, Barsh GS, Schwartz MW (2006) Central nervous system control of food intake and body weight. Nature 443:289-295.
Nieh EH, Vander Weele CM, Matthews GA, Presbrey KN, Wichmann R, Leppla CA, Izadmehr EM, Tye KM (2016) Inhibitory Input from the Lateral Hypothalamus to the Ventral Tegmental Area Disinhibits Dopamine Neurons and Promotes Behavioral Activation. Neuron 90:1286-1298.
Nieh EH, Matthews GA, Allsop SA, Presbrey KN, Leppla CA, Wichmann R, Neve R, Wildes CP, Tye KM (2015) Decoding neural circuits that control compulsive sucrose seeking. Cell 160:528-541.
Palmisano BT, Stafford JM, Pendergast JS (2017) High-Fat Feeding Does Not Disrupt Daily Rhythms in Female Mice because of Protection by Ovarian Hormones. Front Endocrinol (Lausanne) 8:44.
Pinto S, Roseberry AG, Liu H, Diano S, Shanabrough M, Cai X, Friedman JM, Horvath TL (2004) Rapid rewiring of arcuate nucleus feeding circuits by leptin. Science 304:110-115.
Rossi MA (2023) Control of energy homeostasis by the lateral hypothalamic area. Trends Neurosci 46:738-749.
Rossi MA, Stuber GD (2018) Overlapping Brain Circuits for Homeostatic and Hedonic Feeding. Cell Metab 27:42-56.
Rossi MA, Basiri ML, Liu Y, Hashikawa Y, Hashikawa K, Fenno LE, Kim YS, Ramakrishnan C, Deisseroth K, Stuber GD (2021) Transcriptional and functional divergence in lateral hypothalamic glutamate neurons projecting to the lateral habenula and ventral tegmental area. Neuron 109:3823-3837 e3826.
Rossi MA, Basiri ML, McHenry JA, Kosyk O, Otis JM, van den Munkhof HE, Bryois J, Hubel C, Breen G, Guo W, Bulik CM, Sullivan PF, Stuber GD (2019) Obesity remodels activity and transcriptional state of a lateral hypothalamic brake on feeding. Science 364:1271-1274.
Schwartz MW, Woods SC, Porte D, Jr., Seeley RJ, Baskin DG (2000) Central nervous system control of food intake. Nature 404:661-671.
Shi H, Clegg DJ (2009) Sex differences in the regulation of body weight. Physiology & behavior 97:199-204.
Shrivastava K, Swaminathan T, Barlotta A, Athreya V, Choudhry H, Rossi MA (2023) Maternal overnutrition is associated with altered synaptic input to lateral hypothalamic area. Mol Metab 71:101702.
Shrivastava K, Athreya V, Lu Y, Luis-Islas J, Han A, Kowalski TF, Rossi MA (2025) Energy state guides reward seeking via an extended amygdala to lateral hypothalamus pathway. Nat Commun 16:4474.
Siemian JN, Arenivar MA, Sarsfield S, Aponte Y (2021a) Hypothalamic control of interoceptive hunger. Curr Biol 31:3797-3809 e3795.
Siemian JN, Arenivar MA, Sarsfield S, Borja CB, Erbaugh LJ, Eagle AL, Robison AJ, Leinninger G, Aponte Y (2021b) An excitatory lateral hypothalamic circuit orchestrating pain behaviors in mice. Elife 10.
Sim S, Antolin S, Lin CW, Lin Y, Lois C (2013) Increased cell-intrinsic excitability induces synaptic changes in new neurons in the adult dentate gyrus that require Npas4. J Neurosci 33:7928-7940.

Neuroscience Accepted Manuscript

Stamatakis AM, Van Swieten M, Basiri ML, Blair GA, Kantak P, Stuber GD (2016) Lateral Hypothalamic Area Glutamatergic Neurons and Their Projections to the Lateral Habenula Regulate Feeding and Reward. J Neurosci 36:302-311.

Stuber GD, Wise RA (2016) Lateral hypothalamic circuits for feeding and reward. Nat Neurosci 19:198-205.

Stuber GD, Schwitzgebel VM, Luscher C (2025) The neurobiology of overeating. Neuron.

Supiot LF, Kooij KL, Du W, Benschop AAC, Nicolson ASJ, Haak R, Wolterink-Donselaar IG, Luijendijk MCM, Riga D, Adan RAH, Poorthuis RB, Meye FJ (2026) A prefrontal cortex-lateral hypothalamus circuit controls stress-driven increased food intake. Nat Commun.

Thaler JP, Yi CX, Schur EA, Guyenet SJ, Hwang BH, Dietrich MO, Zhao X, Sarruf DA, Izgur V, Maravilla KR, Nguyen HT, Fischer JD, Matsen ME, Wisse BE, Morton GJ, Horvath TL, Baskin DG, Tschop MH, Schwartz MW (2012) Obesity is associated with hypothalamic injury in rodents and humans. The Journal of clinical investigation 122:153-162.

Timper K, Bruning JC (2017) Hypothalamic circuits regulating appetite and energy homeostasis: pathways to obesity. Dis Model Mech 10:679-689.

Toossi H, Del Cid-Pellitero E, Jones BE (2016) GABA Receptors on Orexin and Melanin-Concentrating Hormone Neurons Are Differentially Homeostatically Regulated Following Sleep Deprivation. eNeuro 3.

Turrigiano GG, Leslie KR, Desai NS, Rutherford LC, Nelson SB (1998) Activity-dependent scaling of quantal amplitude in neocortical neurons. Nature 391:892-896.

Ubina T, Vahedi-Hunter T, Agnew-Svoboda W, Wong W, Gupta A, Santhakumar V, Riccomagno MM (2021) ExBoX - a simple Boolean exclusion strategy to drive expression in neurons. J Cell Sci 134.

Valdearcos M, Xu AW, Koliwad SK (2015) Hypothalamic inflammation in the control of metabolic function. Annu Rev Physiol 77:131-160.

Vong L, Ye C, Yang Z, Choi B, Chua S, Jr., Lowell BB (2011) Leptin action on GABAergic neurons prevents obesity and reduces inhibitory tone to POMC neurons. Neuron 71:142-154.

Xue M, Atallah BV, Scanziani M (2014) Equalizing excitation-inhibition ratios across visual cortical neurons. Nature 511:596-600.

Yang Y, Smith DL, Jr., Keating KD, Allison DB, Nagy TR (2014) Variations in body weight, food intake and body composition after long-term high-fat diet feeding in C57BL/6J mice. Obesity (Silver Spring) 22:2147-2155.

Zeltser LM, Seeley RJ, Tschop MH (2012) Synaptic plasticity in neuronal circuits regulating energy balance. Nat Neurosci 15:1336-1342.

Zuloaga DG, Zuloaga KL, Hinds LR, Carbone DL, Handa RJ (2014) Estrogen receptor beta expression in the mouse forebrain: age and sex differences. The Journal of comparative neurology 522:358-371.

JNeurosci Accepted Manuscript

Figure Legends

Figure 1. Sex differences in excitability and synaptic input of LHA^{Vglut2} neurons. (A) Schematic of viral strategy for labeling LHA^{Vglut2} neurons in Vglut2-Cre mice. **(B)** Distribution of recorded LHA^{Vglut2} neurons along the anterior–posterior axis in male and female mice. **(C-D)** Female LHA^{Vglut2} neurons exhibit increased firing in response to depolarizing current injections (two-way ANOVA, main effect of Sex: $F(1, 1869)=53.24$, $p<0.0001$; Current: $F(20, 1869)=120.2$, $p<0.0001$; Interaction: $F(20, 1869)=1.98$, $p=0.006$) and decreased FWHM (t-test, $t(89)=2.45$, $p=0.02$) compared to males (n=40 cells from 3 male mice and n=51 cells from 3 female mice). **(E-K)** Action potential and membrane properties of LHA^{Vglut2} neurons were comparable between male and female mice, including spike threshold (**E;** $t(89)=0.65$, $p=0.52$), action potential rise time (**F;** $t(89)=1.42$, $p=0.16$), afterhyperpolarization (AHP) amplitude (**G;** $t(86)=1.78$, $p=0.078$), resting membrane potential (**H;** $t(89)=0.26$, $p=0.80$), input resistance (**I;** $t(89)=0.42$, $p=0.68$), spontaneous spike rate (**J;** $t(89)=1.63$, $p=0.11$), and rheobase (**K**; $t(89)=0.85$, $p=0.40$). **(L-N)** EPSC frequency ($t(19)=0.63$, $p=0.54$) and amplitude ($t(19)=1.85$, $p=0.08$) were similar between males and females. n=11 cells from 3 male mice and n=10 cells from 2 female mice. **(O-Q)** Female LHA^{Vglut2} neurons displayed increased IPSC frequency compared to males ($t(19)=2.40$, $p=0.027$), while amplitude was unchanged ($t(19)=0.997$, $p=0.33$). n=11 cells from 3 male mice and n=10 cells from 2 female mice. Data are presented as mean ± SEM. $*p<0.05$.

Figure 2. Acute HFD feeding increases LHA^{Vglut2} neuron excitability in male mice. (A) Schematic illustrating viral injection and experimental timeline. Two weeks after surgery, mice were singly housed. One week later, they were randomly assigned to experimental groups and recordings were made from chow-fed controls or after 1-, 2-, or 7-days of HFD feeding. **(B)** Distribution of recorded neurons across anterior–posterior LHA regions under chow and HFD conditions. **(C)** Representative traces of action potential firing in response to depolarizing current injection under chow and HFD conditions. **(D)** Quantification of action potential number as a function of injected current. HFD feeding significantly increased firing compared to chow-fed controls (two-way ANOVA, main effect of Diet: $F(3, 2142)=49.69$, $p<0.0001$ and Current: $F(20, 2142)=130.9$, $p<0.0001$; Interaction: $F(60, 2142)=1.48$, $p=0.01$). Data are presented as mean ± SEM. **(E)** Representative traces showing LHA^{Vglut2} neuron firing in response to +200 pA current ramp. **(F)** Rheobase was reduced in males following HFD feeding (one-way ANOVA, $F(3, 102)=5.57$, $p=0.001$). (**G-K**) Additional electrophysiological parameters of LHA^{Vglut2} neurons showed minimal changes across HFD feeding in male mice. (**G**) FWHM of action potentials ($F(3,$

Neurosci Accepted Manuscript

102)=1.62, p=0.19), (**H**) Spike threshold (F(3, 102)=2.82, p=0.043), (**I**) resting membrane potential (F(3, 102)=0.92, p=0.43), (**J**) input resistance (F(3, 102)=2.3, p=0.08), and (**K**) spontaneous firing rate (F(3, 102)=2.31, p=0.08). Chow: n=40 cells from 3 male mice; HFD1d n=18 cells from 3 male mice; HFD2d: n=23 cells from 3 male mice; HFD7d: n=25 cells from 3 male mice. *Post hoc* tests compared each group to the chow condition. *p<0.05, **p<0.01, ***p<0.001, ****p<0.0001.

Figure 3. Acute HFD feeding does not alter LHA^{Vglut2} neuron excitability in female mice. (A) Schematic illustrating viral injection and experimental timeline. Two weeks after surgery, mice were singly housed. One week later, they were randomly assigned to experimental groups and recordings were made from chow-fed controls or after 1-, 2-, or 7-days of HFD feeding. **(B)** Distribution of recorded neurons across anterior–posterior LHA regions under chow and HFD conditions in female mice. **(C)** Representative traces of action potential firing in response to depolarizing current injection under chow and HFD conditions. **(D)** Quantification of action potential number as a function of injected current. HFD feeding did not significantly alter firing compared to chow in female mice (two-way ANOVA, no main effect of Diet: F(3, 127)=0.50, p=0.68, main effect of Current: F(20, 2540)=426.7, p<0.0001; no Interaction: F(60, 2540)=0.2838, p=0.995). Data are presented as mean ± SEM. **(E)** Representative traces showing LHA^{Vglut2} neuron firing in response to +200 pA current ramp. **(F)** Rheobase in female mice across dietary conditions. One-way ANOVA revealed a significant effect of Diet (F(3, 126)=3.00, p=0.03), but Dunnett's *post hoc* comparisons did not identify significant differences between chow and HFD groups. **(G-K)** Additional electrophysiological parameters of LHA^{Vglut2} neurons showed minimal changes across HFD feeding in female mice. (**G**) FWHM (F(3, 126)=0.90, p=0.44), (**H**) spike threshold (F(3, 126)=6.70, p=0.0003), (**I**) resting membrane potential (F(3, 126)=2.57, p=0.06), (**J**) input resistance (F(3, 126)=0.40, p=0.75), and (**K**) spontaneous spike rate (F(3, 126)=0.47, p=0.70). Chow: n=51 cells from 3 female mice; HFD1d: n=22 cells from 3 female mice; HFD2d: n=28 cells from 3 female mice; HFD7d n=29 cells from 3 female mice. Sidak's *post hoc* test: ∗∗p<0.01, ns: not significant.

Figure 4. Acute HFD feeding differentially regulates synaptic inputs onto LHA^{Vglut2} neurons in males and females. (A) Representative EPSC traces in males under chow and HFD conditions. **(B-C)** In males, HFD reduced EPSC frequency relative to chow (one-way ANOVA, F(3, 53)=3.28, p=0.03), whereas EPSC amplitude showed a significant overall effect (F(3, 53)=4.19, p=0.01); however, Dunnett's *post hoc* comparison revealed no differences between

JNeurosci Accepted Manuscript

chow and the HFD conditions (p>0.05). **(D)** Representative IPSC traces in males under chow and HFD conditions. **(E-F)** In males, IPSC frequency showed a significant overall effect of Diet (F(3, 52)=3.83, p=0.02); however, Dunnett's *post hoc* comparison revealed no differences between chow and the HFD conditions (p>0.05). IPSC amplitude was not significantly altered (F(3, 52)=1.77, p=0.17). Chow: n=11 cells from 2 mice; HFD1d: n=15 cells from 2 mice; HFD2d: n=17 cells from 2 mice; HFD7d: n=14 cells from 2 mice. **(G)** Representative EPSC traces in females under chow and HFD conditions. **(H-I)** In females, HFD did not alter EPSC frequency (F(3, 28)=0.12, p=0.95) or amplitude (F(3, 28)=1.36, p=0.27). **(J)** Representative IPSC traces in females under chow and HFD conditions. **(K-L)** In females, HFD reduced IPSC frequency (F(3, 28)=5.42, p=0.005) and transiently reduced IPSC amplitude at HFD1d (F(3, 28)=3.61, p=0.025). Chow: n=10 cells from 2 mice; HFD1d: n=6 cells from 2 mice; HFD2d: n=8 cells from 2 mice; HFD7d: n=8 cells from 2 mice. Data are presented as mean ± SEM. $*p < 0.05$; $**p < 0.01$.

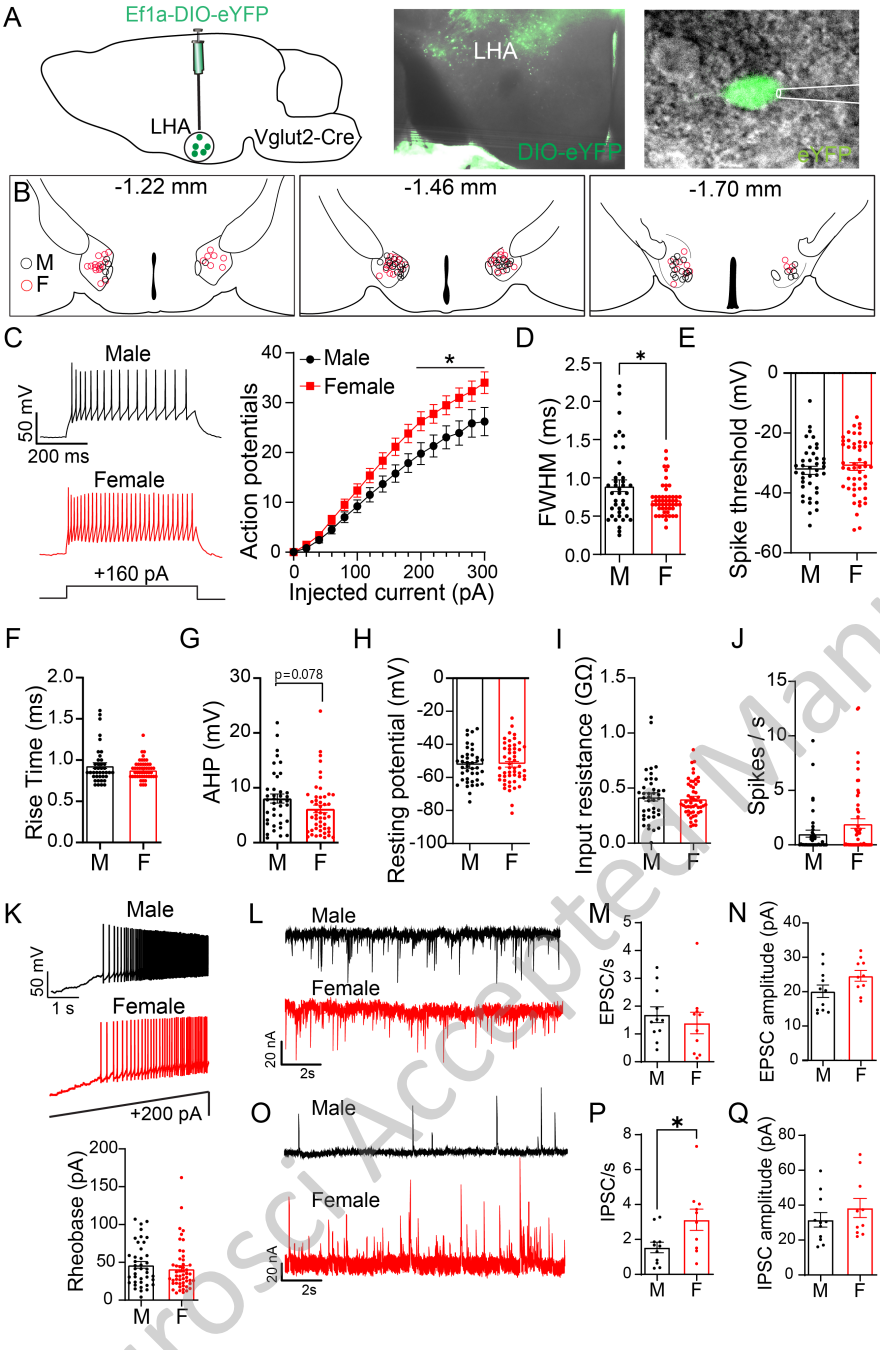
Figure 5. Increasing intrinsic excitability of LHA^{Vglut2} neurons sex-dependently suppresses weight gain. (A) Schematic of viral strategy for NaChBac expression in LHA^{Vglut2} neurons. To express NaChBac in LHA^{Vglut2} neurons, Vglut2-Cre mice were injected in the LHA with Cre-dependent FlpO and Flp-dependent NaChBac. Controls were injected with Cre-dependent eYFP and Flp-dependent NaChBac. Representative injection sites are shown. **(B)** NaChBac expression reduced rheobase (**B**: two-way ANOVA, no main effect of Sex: F(1, 57)=1.09, p=0.30; main effect of Group: F(1, 57)=8.06, p=0.006; no Interaction: F(1, 57)=0.24, p=0.63), action potential threshold (**C**: no main effect of Sex: F(1, 57)=0.05, p=0.82; main effect of Group: F(1, 57)=4.17, p=0.046; no Interaction: F(1, 57)=0.60, p=0.44), and increased total depolarization time after spiking in response to current injection (**D**: no main effect of Sex: F(1, 57)=0.01, p=0.92; main effect of Group: F(1, 57)=10.21, p=0.0023; no Interaction: F(1, 57)=0.01, p=0.92). n=11 cells from 4 male control mice and n=22 cells from 6 male NaChBac mice. n=13 cells from 3 female control mice and n=15 cells from 4 female NaChBac mice. **(E-N)** Effects of NaChBac expression on body weight in males and females under chow and HFD conditions. **(E)** In males maintained on chow diet, NaChBac expression reduced body weight gain (two-way ANOVA, no main effect of Day: F(7, 96)=0.41, p=0.89; main effect of Group: F(1, 96)=37.33, p<0.0001; Interaction: F(7, 96)=3.36, p=0.003). n=7 mice per group. **(F)** Body weight change across the experiment shows a significant reduction in male NaChBac mice compared to controls (t(12)=3.52, p=0.004). n=7 mice per group. **(G)** In females maintained on chow diet, NaChBac expression did not significantly alter body weight gain (two-way ANOVA, no main effect of Day: F(7, 112)=1.72, p=0.11; no main effect of

JNeurosci Accepted Manuscript

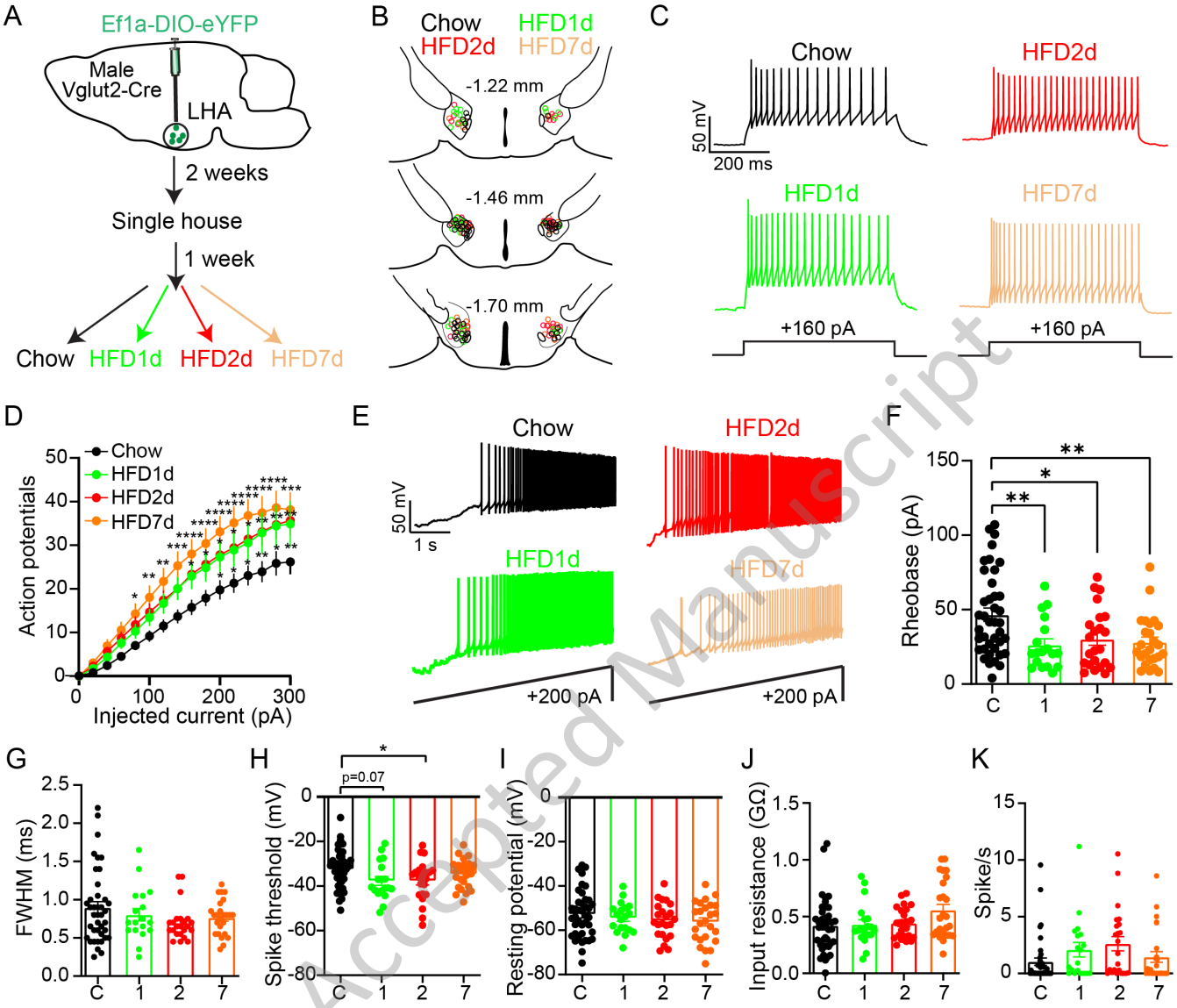
Group: F(1, 112)=0.30, p=0.59; no Interaction: F(7, 112)=0.32, p=0.94). n=8 mice per group. **(H)** Body weight change in females shows no significant difference between NaChBac and controls (t(14)=0.91, p=0.38). n=8 mice per group. **(I)** In males maintained on HFD, NaChBac expression reduced body weight gain (no main effect of Day: F(7, 104)=1.56, p=0.15; main effect of Group: F(1, 104)=15.89, p=0.0001; Interaction: F(7, 104)=2.130, p=0.047). n=8 Control and n=7 NaChBac mice. **(J)** NaChBac suppresses body weight gain in males maintained on HFD (t(13)=3.08, p=0.009). n=8 Control and n=7 NaChBac mice. **(K)** In females maintained on HFD, NaChBac expression significantly reduced body weight gain (no main effect of Day: F(7, 112)=0.57, p=0.78; main effect of Group: F(1, 112)=56.73, p<0.0001; Interaction: F(7, 112)=5.95 , p<0.0001). n=6 Control and n=10 NaChBac mice. **(L)** NaChBac produced weight loss in females maintained on HFD (t(14)=5.40, p<0.0001). n=6 Control and n=10 NaChBac mice. **(M–N)** Comparison of male and female body weight change in (**M**) control mice (no main effect of Diet: F(1, 25)=3.78, p=0.06; no main effect of Sex: F(1, 25)=0.24, p=0.63; no Interaction: F(1, 25)= 9.183×10^{-6}, p=0.998) and (**N**) NaChBac-expressing mice (main effect of Diet: F(1, 28)=8.39, p=0.007; main effect of Sex: F(1, 28)=5.59, p=0.025; Interaction: F(1, 28)=13.96, p=0.0008). **(O)** NaChBac expression did not affect 6-h chow intake (no main effect of Group: F(1, 26)= 0.04, p=0.83; no main effect of Sex: F(1, 26)=0.63, p=0.43; no Interaction: F(1, 26)= 2.56, p=0.12). **(P)** NaChBac expression increased HFD intake for both males and females (main effect of Group: F(1, 25)=13.95, p=0.001; no main effect of Sex: F(1, 25)=1.24, p=0.28; no Interaction: F(1, 25)= 1.14, p=0.30). n = 7 male Controls and n = 7 male NaChBac; n = 8 female Controls and n = 8 female NaChBac for chow intake; n = 7 male Controls and n = 6 male NaChBac; n = 7 female Controls and n = 9 female NaChBac for HFD intake. Data are presented as mean ± SEM. Sidak's *post hoc* test: $*p < 0.05$; $**p < 0.01$; $***p < 0.001$, $****p < 0.0001$.

Figure 6. NaChBac expression in LHA^{Vglut2} neurons does not alter anxiety-like behavior. (A-B) Light–dark box test showing time spent in the light zone and number of entries. No significant differences were observed between control and NaChBac groups in males (time: t(12)=0.43, p=0.68; entries: t(12)=2.08, p=0.06) or females (time: t(14)=0.46, p=0.65; entries: t(14)=0.87, p=0.40). **(C-D)** Open field test showing time spent in the center of the arena and total distance traveled. No significant differences between NaChBac and Control mice were observed in males (center time: t(12)=0.51, p=0.62; distance: t(12)=0.35, p=0.73) or females (center time: t(14)=0.35, p=0.73; distance: t(14)=0.12, p=0.91). n=7 male Controls, n=7 male NaChBac, n=8 female Controls, n=8 female NaChBac. Data are presented as mean ± SEM.

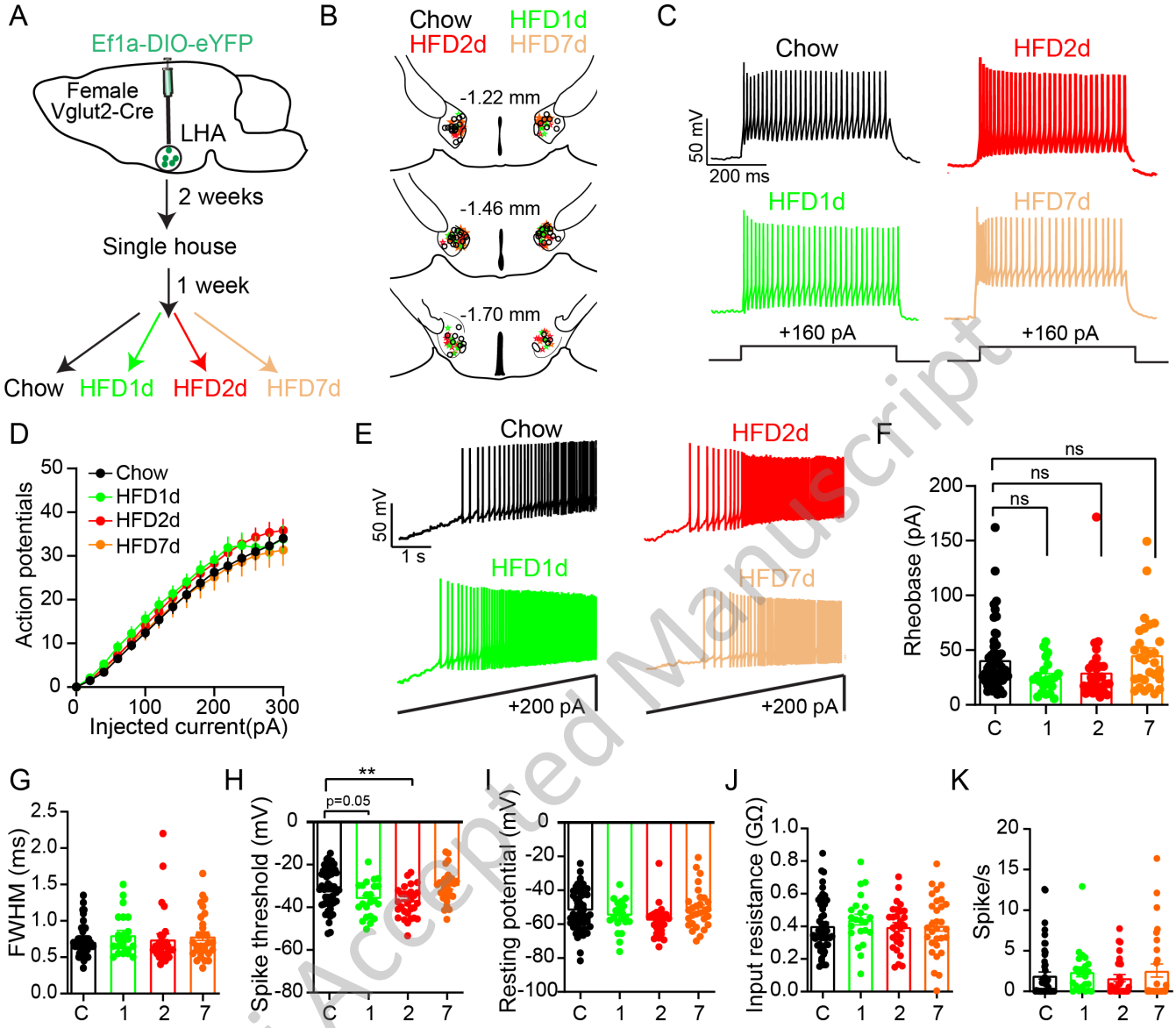
J Neurosci Accepted Manuscript



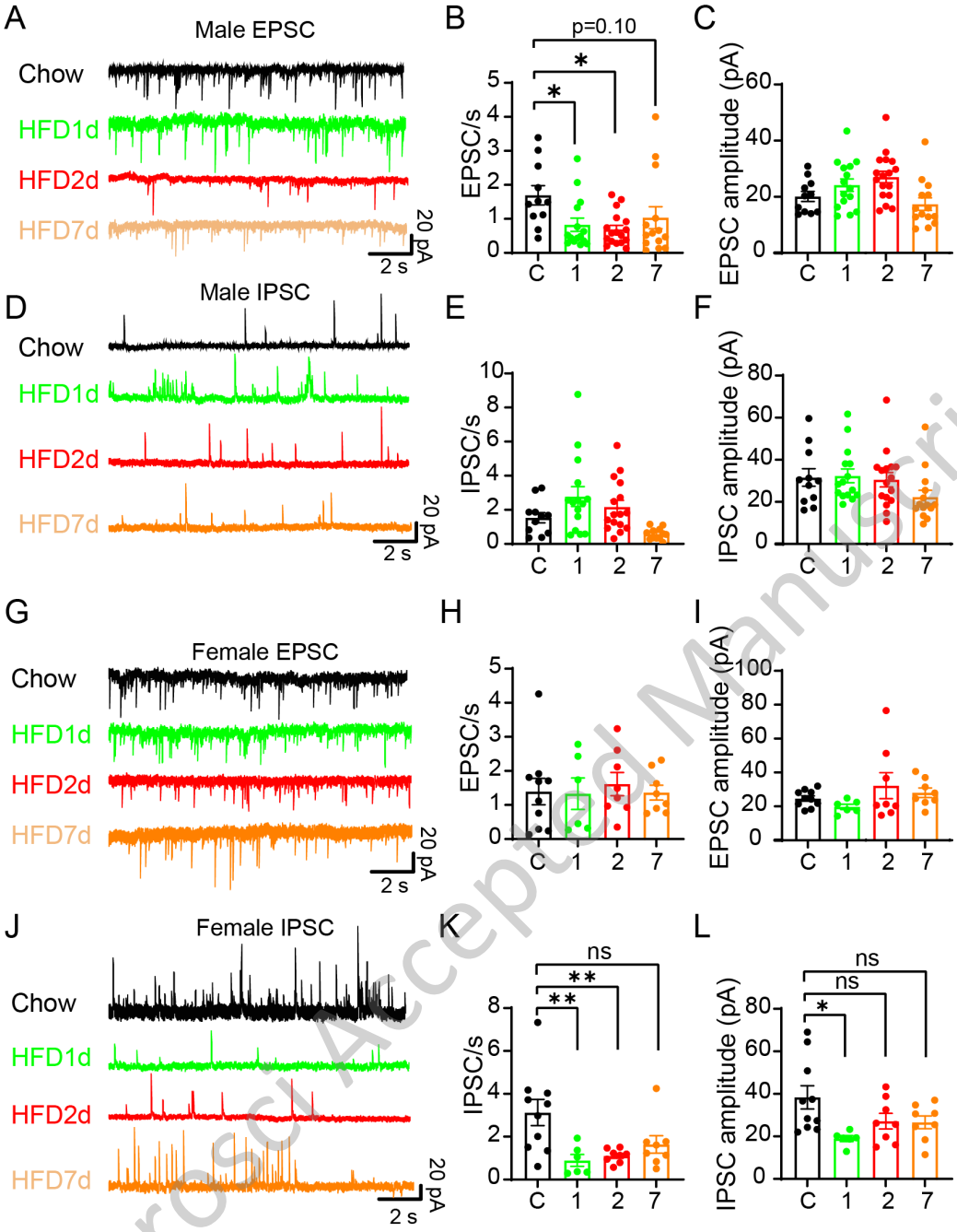
JNeurosci Accepted Manuscript



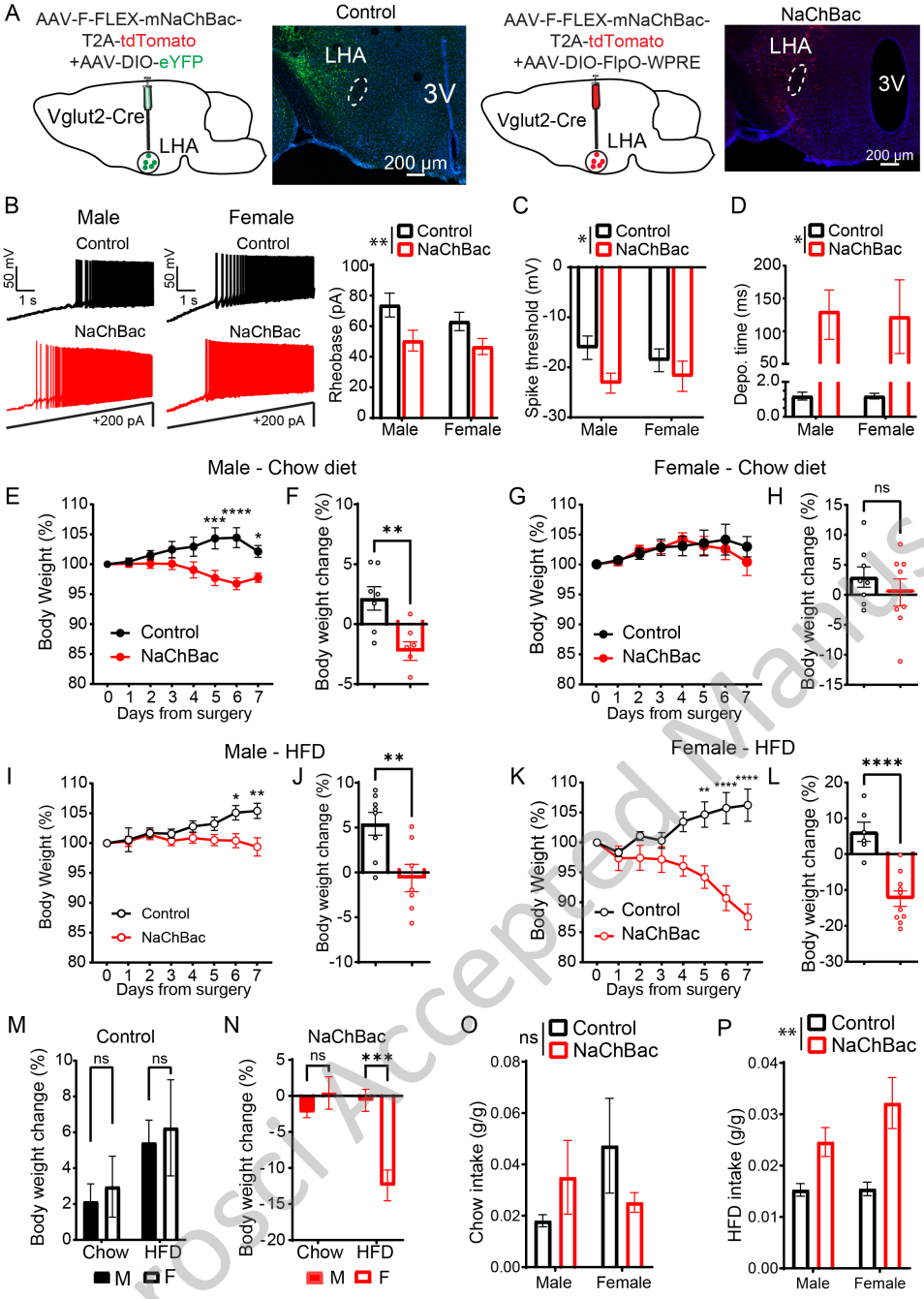
JNeurosci Accepted Manuscript



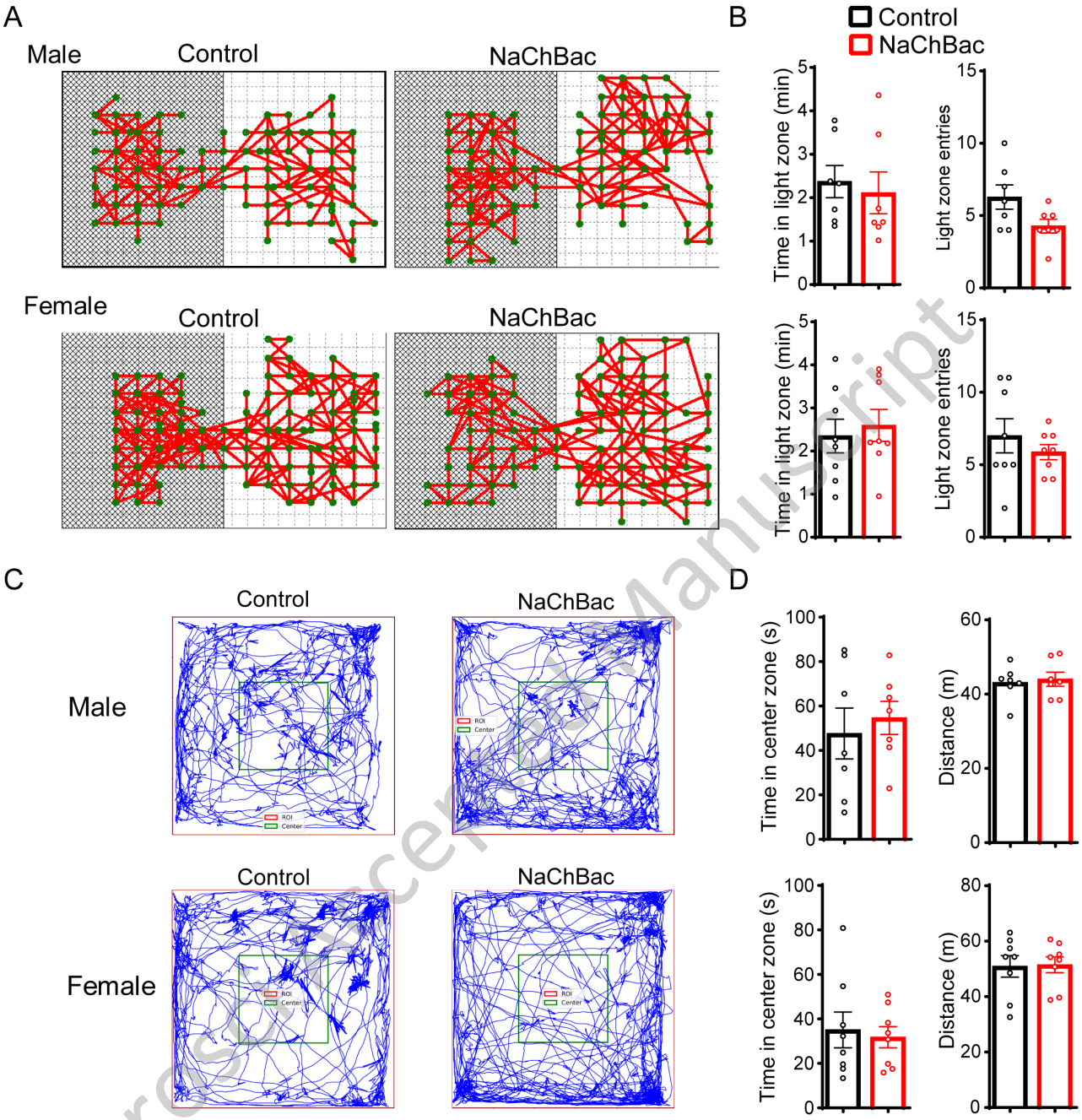
JNeurosci Accepted Manuscript



JNeurosci Accepted Manuscript



JNeurosci Accepted Manuscript



JNeurosci Accepted Manuscript